

RESEARCH ARTICLE SUMMARY

NEUROSCIENCE

Anterior cingulate inputs to nucleus accumbens control the social transfer of pain and analgesia

Monique L. Smith, Naoyuki Asada, Robert C. Malenka*

INTRODUCTION: Empathy, the adoption of another's sensory and emotional state, plays a critical role in social interactions. Although, historically, empathy was often considered to be an affective-cognitive process experienced solely by humans, it is now appreciated that many species, including rodents, display evolutionarily conserved behavioral antecedents of empathy such as observational fear. It is therefore possible

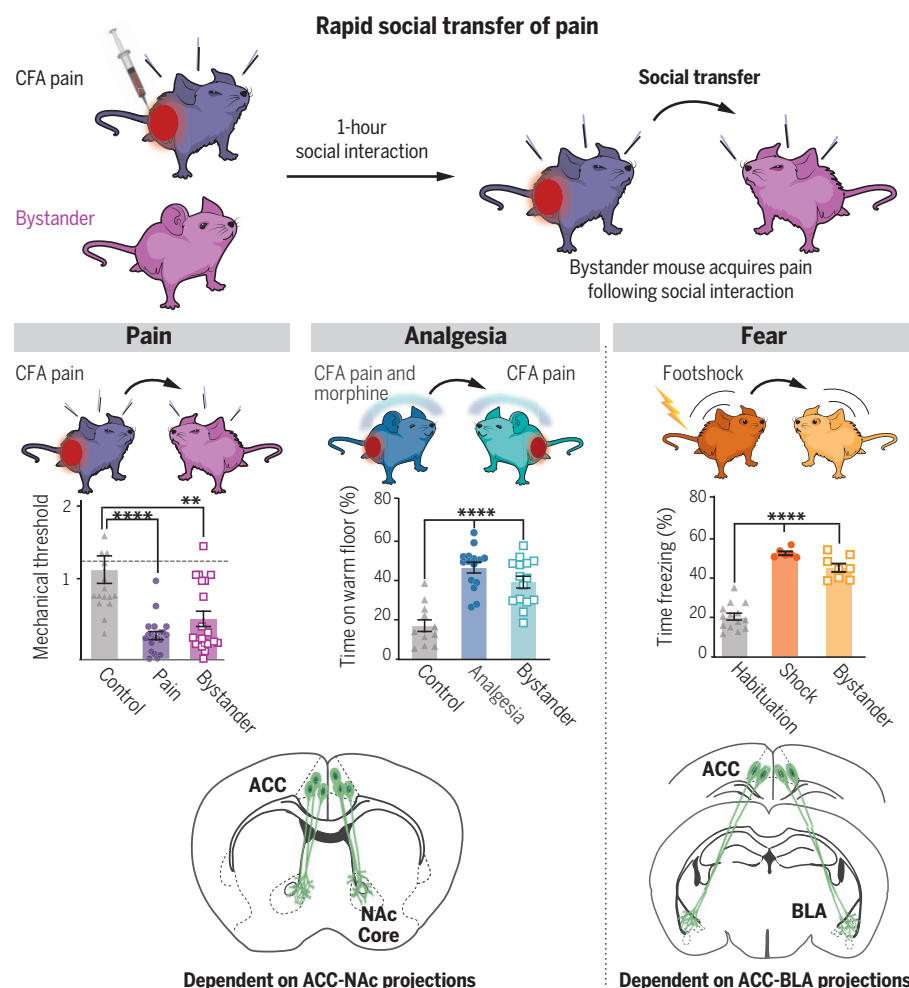
to begin to define the neural mechanisms that mediate behavioral manifestations of empathy in species that are optimal for application of modern circuit neuroscience tools.

RATIONALE: In both humans and rodents, the anterior cingulate cortex (ACC) appears to encode information about the affective state of others. However, little is known about which

downstream targets of the ACC contribute to empathy-related behaviors. To address this topic, we optimized a protocol for the social transfer of pain behavior in mice and compared the ACC-dependent neural circuitry responsible for this behavior with the ACC neural circuitry required for the social transfer of two related behavioral states: analgesia and fear. These behaviors exhibit a key component of empathy, the adoption of another's sensory and affective state.

RESULTS: A 1-hour social interaction between a bystander mouse and a cagemate experiencing inflammatory pain led to mechanical hyperalgesia in the bystander mouse, which lasted 4 hours but not 24 hours. This social transfer of pain was also evident after thermal testing and led to affective changes that were detected by a conspecific. The social interaction led to activation of neurons in the ACC and several downstream targets, including the nucleus accumbens (NAc), which was revealed by monosynaptic rabies virus tracing to be directly connected to the ACC. Bidirectional manipulation of activity in ACC-to-NAc inputs influenced the acquisition of socially transferred pain but not the expression of the mechanical sensitivity used to assay pain thresholds. A behavioral protocol revealed the rapid social transfer of analgesia, which also required activity in ACC-to-NAc inputs. By contrast, ACC-to-NAc input activity was not required for the social transfer of fear, which instead required activity in ACC projections to the basolateral amygdala (BLA).

CONCLUSION: We established that mice rapidly adopt the sensory-affective state of a social partner, regardless of the valence of the information (that is, pain, fear, or pain relief). We find that the ACC generates specific and appropriate empathic behavioral responses through distinct downstream targets. Specifically, ACC-to-NAc input activity is necessary for the social transfer of pain and analgesia but not the social transfer of fear, which instead requires ACC-to-BLA input activity. Elucidating circuit-specific mechanisms that mediate various forms of empathy in experimentally accessible animal models is necessary for generating hypotheses that can be evaluated in human subjects using noninvasive assays. More sophisticated understanding of evolutionarily conserved brain mechanisms of empathy will also expedite the development of new therapies for the empathy-related deficits associated with a broad range of neuropsychiatric disorders. ■



Distinct ACC neural circuits mediate social transfer of pain states and fear. Complete Freund's adjuvant (CFA)-induced pain is transferred from cagemates to bystanders after a 1-hour social interaction. Bystanders also exhibit pain relief after interacting with cagemates that are experiencing pain and morphine analgesia. The social transfer of pain and analgesia both require ACC-to-NAc projections, whereas the social transfer of fear requires ACC projections to the BLA. Data represent mean \pm SEM; dashed line indicates mean baseline threshold for all groups; ** $P < 0.01$ and **** $P < 0.0001$.

The list of author affiliations is available in the full article.

*Corresponding author. Email: malenka@stanford.edu

S READ THE FULL ARTICLE AT
<https://doi.org/10.1126/science.abe3040>

RESEARCH ARTICLE

NEUROSCIENCE

Anterior cingulate inputs to nucleus accumbens control the social transfer of pain and analgesia

Monique L. Smith, Naoyuki Asada*, Robert C. Malenka†

Empathy is an essential component of social communication that involves experiencing others' sensory and emotional states. We observed that a brief social interaction with a mouse experiencing pain or morphine analgesia resulted in the transfer of these experiences to its social partner. Optogenetic manipulations demonstrated that the anterior cingulate cortex (ACC) and its projections to the nucleus accumbens (NAc) were selectively involved in the social transfer of both pain and analgesia. By contrast, the ACC→NAc circuit was not necessary for the social transfer of fear, which instead depended on ACC projections to the basolateral amygdala. These findings reveal that the ACC, a brain area strongly implicated in human empathic responses, mediates distinct forms of empathy in mice by influencing different downstream targets.

Empathy plays an essential role in social communication and involves integrated behavioral, cognitive, and affective processes that facilitate the adoption of a sensory or affective state that is more appropriate to another's situation than one's own (1–3). Evolutionarily conserved behavioral antecedents of human empathy have been identified in a range of species (2–5), including rodents, which display emotional contagion (6, 7), socially transferred pain (8–11), observational fear (3, 5, 12), and prosocial behaviors such as consolation (13) and “helping” (14, 15).

The anterior cingulate cortex (ACC) is a principal node in the neural circuitry thought to mediate empathy (16–18). In both humans and rodents, the ACC is particularly critical for affective and motivational responses to direct and observed pain as well as the social transfer of pain (10, 13, 19, 20). The ACC is thought to communicate with a broad range of brain regions that regulate emotional and motivational states, including the thalamus, insula, amygdala, and nucleus accumbens (NAc) (16, 21–23). However, the roles of these specific ACC circuit elements in empathy-related behaviors are unknown.

Rapid transfer of pain behavior to bystander mice

The presence of a conspecific in pain can modulate the expression of pain behavior in a test animal already experiencing pain (6) and cause hyperalgesia in “bystander” (BY) mice that have not been subjected to any pain-inducing stimuli (9, 10), a phenomenon known as the “social transfer of pain.” We examined whether

a brief (1 hour), direct social interaction between a male BY mouse and a male cagemate experiencing inflammatory hyperalgesia [owing to intraplantar injection of complete Freund's adjuvant (CFA), which induces long-lasting arthritis-like pain, (24, 25)] would lead to the social transfer of pain (Fig. 1A). After this 1-hour social interaction, BY mice exhibited mechanical hypersensitivity [as measured by stimulation with von Frey hairs using the “up-down” technique (26)] equivalent to that of CFA mice, whereas control mice subjected to the same procedures (in the absence of a no-ciceptive stimulus in either mouse) exhibited no change in mechanical thresholds (Fig. 1, B and C). After von Frey testing, all mice were separated and housed with treatment-matched cagemates (fig. S1). Repeated mechanical testing revealed that the hyperalgesia in BY mice lasted 4 hours but not 24 hours (Fig. 1B), was not influenced by prolonging the social interaction to 2 hours (fig. S2A) or by delaying the start of the social interaction to 24 hours after CFA injection (fig. S2B), and still occurred when capsaicin was used to induce pain and the social interaction was limited to 30 min (fig. S2C). Females demonstrated similar social transfer of pain (fig. S3A), although they expressed lower basal mechanical thresholds and enhanced CFA-induced hypersensitivity (fig. S3, A to C).

Whereas CFA mice exhibited hyperalgesia only in the ipsilateral, CFA-injected hindpaw, BY mice exhibited hyperalgesia in both hindpaws (Fig. 1D), suggesting the involvement of higher brain regions in mediating the pain transfer. Both CFA and BY mice also displayed thermal hypersensitivity to tail immersion in hot water (Fig. 1E) and thermal place aversion when given the choice between a warm (40°C) or room temperature (30°C) floor in a thermal place test (TPT; Fig. 1F). To determine whether

the socially transferred pain experienced by BY mice led to affective changes that could be detected by a conspecific, we conducted an emotional discrimination task (27), which demonstrated that a stranger mouse spent more time exploring both CFA and BY mice compared with controls (Fig. 1G).

Activation of an ACC-to-NAc core circuit by the social transfer of pain

To elucidate the brain regions potentially contributing to the social transfer of pain, we identified neurons activated during the social interaction using a reporter line generated by crossing FosCreER^{T2} (TRAP2) mice with the Ai14-TdTomato reporter line (28, 29). Administering 4-hydroxytamoxifen (4-OHT) immediately before a 4-hour social interaction between BY and CFA mice (Fig. 2A) generated activated neurons in BY mice in brain regions previously associated with empathy and social motivation, such as the ACC and NAc, as well as regions associated with pain transmission, such as the thalamus, central amygdala, and periaqueductal gray (Fig. 2, B and C). Because the numbers of activated neurons in the ACC and NAc were greater in BY mice than in both control and CFA mice (Fig. 2C) and because the ACC and NAc are important for social behaviors (30–33), we hypothesized that ACC neurons synapse onto NAc cells that are activated during the social transfer of pain. Thus, we first injected AAV-CaMKIIα-YFP (AAV, adeno-associated virus; YFP, yellow fluorescent protein) into the ACC and verified that ACC pyramidal neurons send projections to the NAc, preferentially in its core region (Fig. 2D). To determine if there are direct synaptic connections between ACC neurons and activated NAc neurons during social transfer, we applied monosynaptic rabies virus tracing (34, 35) in TRAP2-BY and -CFA mice. Injection of AAVs expressing Cre-dependent rabies glycoprotein (RG) and avian tumor virus receptor A (TVTA) into the NAc core followed by injection of EnvA-pseudotyped RG-deleted rabies virus expressing green fluorescent protein (GFP) (Fig. 2E), resulted in similar levels of GFP expression throughout the ACC in both CFA and BY mice (Fig. 2F and fig. S4).

ACC-to-NAc projections bidirectionally control social transfer of pain

To investigate if the ACC→NAc pathway is required for the social transfer of pain, we first tested the necessity of the ACC itself by injecting AAVs expressing the inhibitory opsin halorhodopsin (NpHR; AAV-DJ-CaMKIIα-NpHR) or enhanced YFP (eYFP) as a control (YFP; AAV-DJ-CaMKIIα-eYFP) and placing an optical fiber directly above the ACC (Fig. 3A). Activating NpHR during the social interaction between BY and CFA mice (Fig. 3A) attenuated the hyperalgesia in BY mice but not CFA mice,

Nancy Pritzker Laboratory, Department of Psychiatry and Behavioral Sciences, Stanford University, Stanford, CA, USA.

*Present address: Daiichi Sankyo Co., Ltd., Tokyo, Japan.

†Corresponding author. Email: malenka@stanford.edu

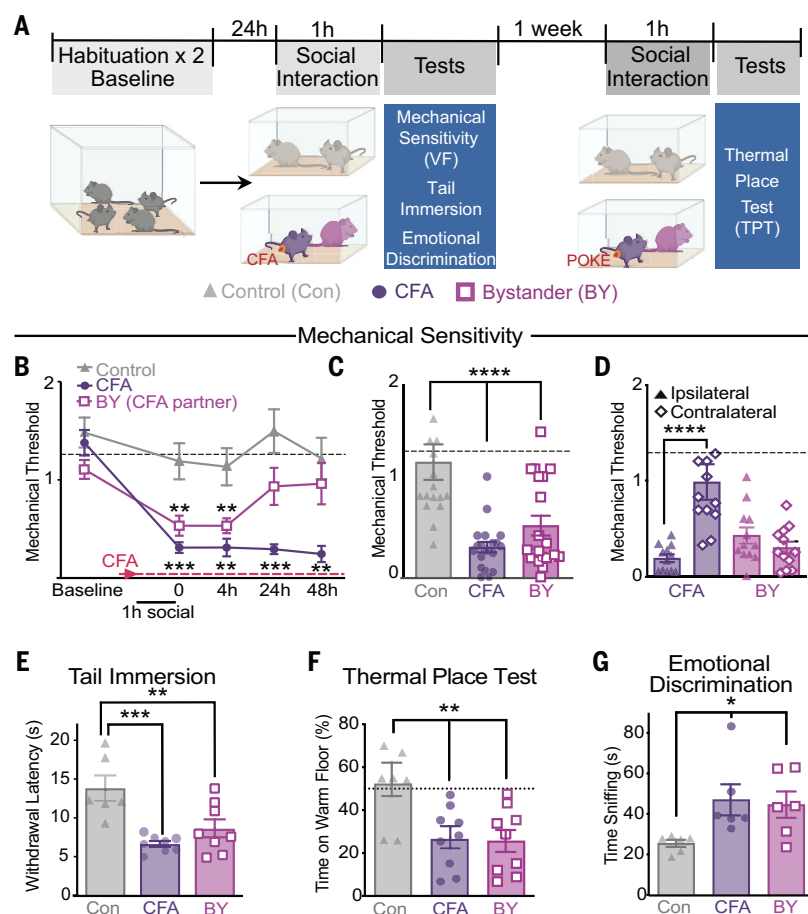


Fig. 1. Rapid social transfer of pain to bystander mice. (A) Timeline of social transfer of pain protocol. h, hour(s). (B) Time course of mechanical von Frey (VF) sensitivity at 0, 4, 24, and 48 hours after 1-hour social interaction in Control-Control (Con-Con) and CFA-BY pairs. (C) Mechanical thresholds immediately after the 1-hour social interaction. (D) Mechanical thresholds of the ipsilateral versus contralateral hindpaws. (E) Tail withdrawal latencies in the tail immersion test. (F) Time spent on the warm floor (40°C) in the TPT. (G) Time a stranger conspecific spent sniffing each group. For (B) to (G), data are means \pm SEM. In (B) to (D), dashed lines represent mean baseline thresholds for all groups. In (F), the dotted line represents 50% time on warm floor. Statistical tests included two-way repeated measures (A), one-way [(B) and (E) to (G)], and two-way (D) analysis of variance (ANOVA) with Holm-Sidak post hoc tests; * $P < 0.05$, ** $P < 0.01$, *** $P < 0.001$, and **** $P < 0.0001$ representative of post hoc comparisons. All statistical measure details are presented in table S1A.

whereas YFP-expressing BY and CFA mice exposed to the same light stimulation displayed the expected mechanical hypersensitivity (Fig. 3B). Acute light exposure in the same mice during the mechanical testing had no consistent effect on mechanical thresholds (Fig. 3C), suggesting that acute inhibition of ACC neurons does not directly alter mechanical sensation.

To determine if the subset of ACC neurons activated during an initial social interaction is necessary for subsequent socially transferred pain, TRAP2: Ai14 mice that had received ACC injections of AAV-DIO-NpHR or AAV-DIO-eYFP were given 4-OHT before the social transfer of pain. One week later, optogenetic inhibition of the TRAPed ACC neurons during a second social interaction prevented BY mice from developing mechanical hypersensitivity

compared with control YFP-BY mice, which expressed robust hyperalgesia (Fig. 3D). Immediately after the initial light-off test, the same mice were given light stimulation of the TRAPed neurons during the mechanical testing, and this manipulation had no consistent effect (Fig. 3E).

We next tested the necessity of ACC→NAC projections specifically by bilaterally injecting NpHR- or YFP-expressing AAVs in the ACC and placing optical fibers immediately above the NAc core. Similar to the effects of inhibiting the ACC, inhibition of ACC→NAC projections during the 1-hour social interaction strongly impaired the social transfer of mechanical hypersensitivity to BY mice but had no effects on CFA mice or YFP-expressing BY and CFA mice (Fig. 3F). Furthermore, repeated inhibition

of the ACC→NAC projections during mechanical testing in the same mice had no consistent effect on mechanical thresholds (Fig. 3G).

To further evaluate the role of the ACC→NAC pathway in the social transfer of pain, we expressed channelrhodopsin-2 (ChR2) in the ACC and activated ACC→NAC projections during the 1-hour social transfer. This caused a robust prolongation of the duration of hyperalgesia in the BY mice, which lasted >72 hours as opposed to the expected 4 to 24 hours, as seen in YFP-expressing BY mice (Fig. 3H). Before any nociceptive stimulation, acute activation of ACC→NAC projections during mechanical testing had no consistent effect on mechanical sensitivity (fig. S5A) and also did not have acute aversive or reinforcing effects, as assayed by a real-time place preference test (fig. S5B).

Distinct ACC projections control the social transfer of pain and fear

To examine the generalizability of ACC→NAC control over socially transferred behaviors, we examined the role of ACC→NAC projections in the well-established phenomenon of the social transfer of fear (5, 12). BY mice were exposed to shock 24 hours before placement in a distinct context, which allowed observation of a demonstrator (Shock) mouse being repeatedly shocked (Fig. 4A). Shock pre-exposure enhances the magnitude of freezing behavior in BY mice and is thought to more closely model human empathy (12, 20, 36). During the short observation period, BY mice exhibited significant increases in freezing (Fig. 4B), and this was maintained 24 hours later during reexposure to the shock observation context (“retrieval”; Fig. 4C). Inhibition of ACC→NAC projections in BY mice during the conditioning phase (Fig. 4D) had no effect on their acquisition of freezing behavior (Fig. 4E) and also did not affect freezing during the context-induced retrieval (Fig. 4F), where light was applied every other minute (fig. S6A). However, when the same mice were subjected to the social transfer of pain, inhibition of the ACC→NAC projections during a 1-hour social interaction between CFA and BY mice impaired the acquisition of hyperalgesia in the BY mice (Fig. 4G), thereby providing evidence that the optogenetic inhibition of ACC→NAC input activity was effective in these mice.

ACC projections to the basolateral amygdala (BLA) are necessary for cue-induced retrieval of socially transferred fear (36). To evaluate if ACC→BLA projections are also necessary for context-induced retrieval of socially transferred fear behavior, we inhibited this pathway during acquisition of socially transferred fear and intermittently during retrieval (Fig. 4D). Inhibition of ACC→BLA projections in BY mice had no effect on their acquisition of freezing

behavior (Fig. 4H) but did attenuate freezing behavior during retrieval (Fig. 4I), regardless of whether the light was on or off (fig. S6B). By contrast, when the same mice were tested for the social transfer of pain, there was no effect of ACC→BLA input inhibition during the social interaction on their mechanical thresholds (Fig. 4J).

ACC-to-Nac projections regulate the social transfer of analgesia

Although the social transfer of pain and fear in rodents is well established, it is unknown if the experience of pain relief [i.e., analgesia (Analg)] can be transferred socially. To examine this possibility, all mice were administered CFA to induce pain and then one-quarter of mice were also given an analgesic dose of morphine [10 mg per kg of body weight (mg/kg)] at which time mice were paired for a 1-hour social interaction (Fig. 5A). Despite prior administration of CFA, CFA-Analg-BY mice paired with morphine-treated mice (CFA-Mor) exhibited diminished reductions in mechanical threshold (i.e., lessened pain responses) compared with CFA-CFA control pairs (CFA-Con; Fig. 5B). After separation from CFA-Mor partners, the social transfer of analgesia in CFA-Analg-BY mice lasted 4 hours but not 24 hours (Fig. 5B). Because morphine causes hyperlocomotion, which prevents measurement of mechanical thresholds in CFA-Mor mice, we used the TPT to directly compare the magnitude of the analgesia in CFA-Analg-BY and CFA-Mor mice. In contrast to mechanical hyperalgesia, thermal place aversion was not present 1 hour after CFA injection but was robust 1 week later (Fig. 5C), at which point one-quarter of CFA mice were again administered morphine immediately before a 1-hour social interaction with CFA-Analg-BY partners (Fig. 5A). CFA-induced thermal aversion (CFA-Con) was reduced in the CFA-Analg-BY mice to the same extent as morphine administration (CFA-Mor; Fig. 5D).

We next tested the necessity of ACC activity for the social transfer of analgesia. Optogenetic inhibition of ACC neurons using NpHR during the 1-hour social interaction (Fig. 5E) prevented the social transfer of analgesia in CFA-Analg-BY mice, as assayed by both mechanical sensitivity (Fig. 5F) and the TPT (Fig. 5G), but had no effect on acute mechanical thresholds, thermal place aversion, or the analgesic action of morphine during the testing of CFA-Con and CFA-Mor mice. Inhibition of ACC→Nac input activity specifically had essentially identical effects, also preventing the social transfer of analgesia without affecting mechanical or thermal sensitivity directly (Fig. 5, H and I).

Discussion

We investigated the neural mechanisms of simple forms of empathy in mice by establishing

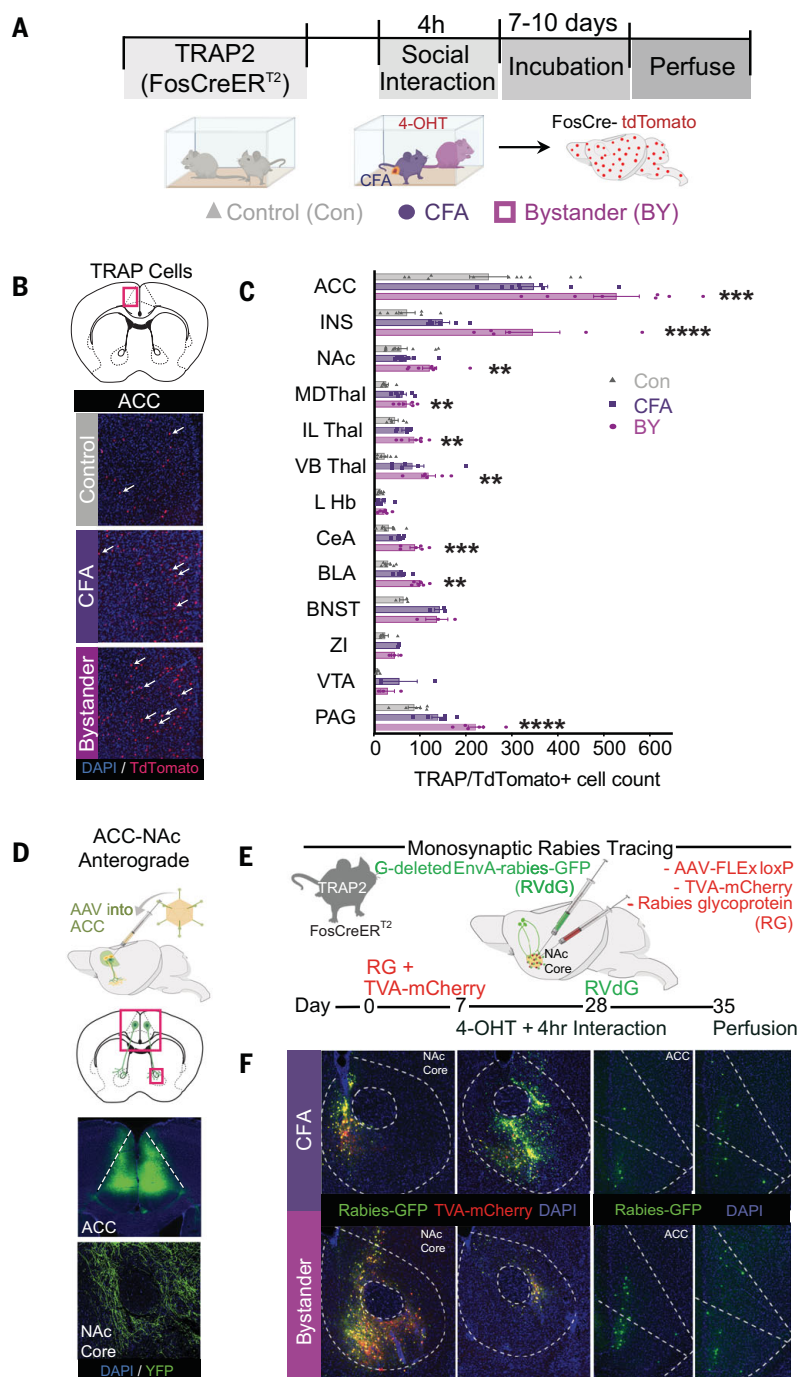


Fig. 2. Activation of an ACC Nac core circuit by the social transfer of pain. (A) Timeline to “TRAP” activated neurons during social transfer of pain. (B) Representative photomicrographs of TdTomato-positive cells (white arrows) in the ACC of Con, CFA, and BY mice after social transfer of pain. The red rectangle indicates the location of the photomicrographs. DAPI, 4',6-diamidino-2-phenylindole. (C) Quantification of Ai14-positive-TRAPed cells across 13 brain regions (n = 6 to 9 mice per group). (D) Schematic of AAV injection and representative photomicrographs of ACC injection site and fibers in the Nac core. The large and small red rectangles indicated the location of the top and bottom micrographs, respectively. The dashed white lines indicate boundaries of the ACC. (E) Schematic and timeline of monosynaptic rabies tracing. (F) Representative photomicrographs of Nac core G-deleted EnvA-rabies-GFP (RVdG) and RG injection site and ACC GFP expression in CFA and BY mice. The dashed lines indicate boundaries of the Nac core and ACC. Data are means ± SEM; one-way ANOVA with Holm-Sidak post hoc tests comparing Con versus BY; **P < 0.01, and ***P < 0.001, and ****P < 0.0001. All statistical measure details are presented in table S1B. INS, insula; MD Thal, mediodorsal thalamus; IL Thal, interlaminar thalamus; VB Thal, ventrobasal thalamus; L Hb, lateral habenula; CeA, central amygdala; BLA, basolateral amygdala complex; BNST, bed nucleus of the stria terminalis; ZI, zona inserta; VTA, ventral tegmental area; PAG, periaqueductal gray.

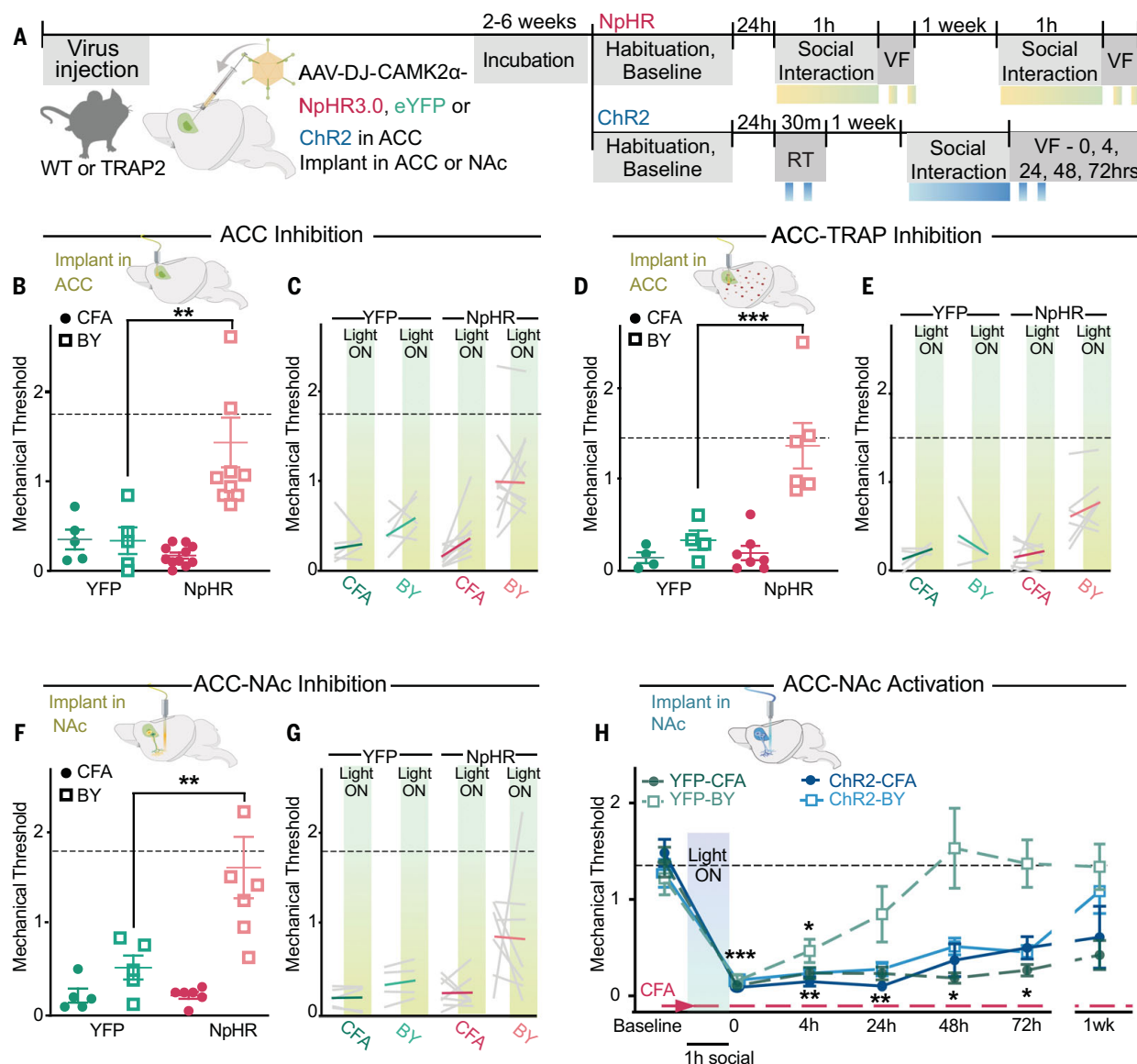


Fig. 3. ACC NAc projections bidirectionally control social transfer of pain.

(A) Schematic of viral injection and experimental timeline. Light stimulation periods are represented by yellow-green boxes for NpHR activation and by blue boxes for ChR2 activation. RT, real-time place preference. (B) Schematic shows fiber optic implant above the ACC. First light-off test of mechanical sensitivity (VF) of YFP- and NpHR-injected mice immediately after 1-hour social transfer with ACC inhibition. (C) Mechanical sensitivity during averaged ($n = 2$) light-off and light-on sessions of ACC inhibition. (D) Schematic shows fiber optic implant above the ACC. First light-off test of mechanical sensitivity of YFP- and NpHR-injected TRAP2 mice immediately after 1-hour social transfer with ACC-TRAP inhibition. (E) Mechanical sensitivity during averaged ($n = 2$) light-off and light-on sessions of ACC-TRAP inhibition. (F) Schematic of bilateral fiber

optic implants above the NAc core. First light-off test of mechanical sensitivity of YFP- and NpHR-injected mice immediately after 1-hour social transfer with ACC→NAC input inhibition. (G) Mechanical sensitivity during averaged ($n = 2$) light-off and light-on sessions of ACC→NAC input inhibition. (H) First light-off test of mechanical sensitivity at 0, 4, 24, 48, and 72 hours and 1 week after 1-hour social interaction with ACC→NAC input inhibition. Data are means \pm SEM. Dashed lines represent mean baseline thresholds for all groups. One-way ANOVA with Holm-Sidak post hoc tests comparing YFP to matched NpHR groups [(B) to (G)] and two-way repeated measures ANOVA with Holm-Sidak post hoc tests comparing treatment groups to baseline at each time point, where notation is the least significant P value of all comparisons (H); * $P < 0.05$, ** $P < 0.01$, and *** $P < 0.001$. All statistical measure details are presented in table S1C.

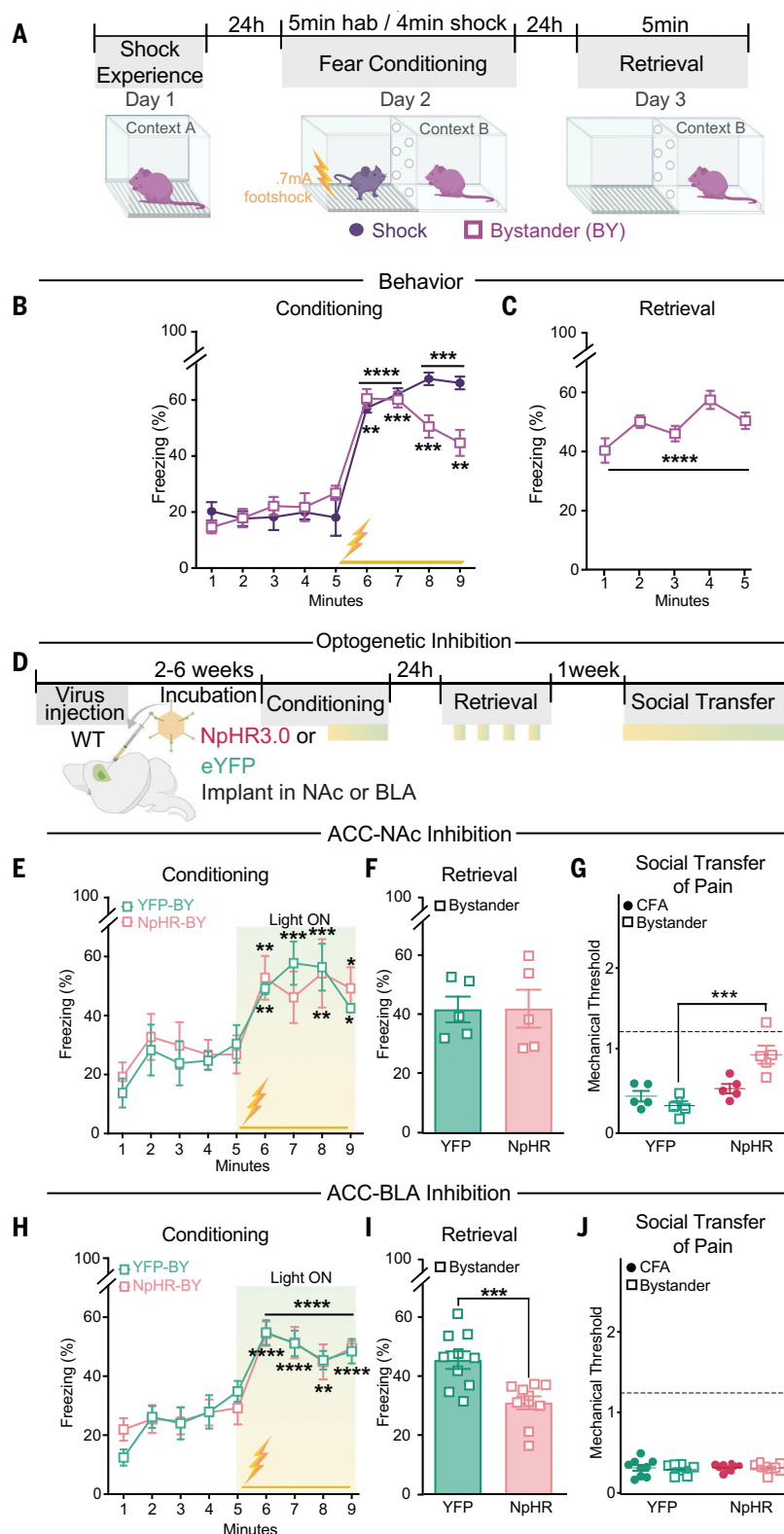
a protocol that results in the rapid social transfer of two types of pain behavior: hyperalgesia and analgesia. Although the definition of “empathy” is subject to debate (37), the BY mice in this bidirectional behavioral model appear to fulfill one critical feature of the expression of empathy, the adoption of another’s sensory and affective state (1–3, 37). The social transfer

of hyperalgesia to BY mice required only 1 hour of social interaction, lasted 4 to 24 hours, and generalized to several different pain modalities. Notably, analgesia could also be transferred to a mouse in pain and lasted at least 4 hours. These results provide further evidence for the critical importance of the social environment to the experience of pain, including an inno-

vative model for socially induced pain relief, which can be tested in human subjects.

The social interactions in mice resulted in increased activity in the ACC and several of its downstream targets, such as the NAc, a key node of the circuitry involved in a range of affective and motivated behaviors, including those triggered by pain (38–41). A critical role

Fig. 4. Distinct ACC projections control the social transfer of pain and fear. (A) Schematic and timeline of social transfer of fear (shock experience: two at 0.7 mA, 2-s duration, 1-min intervals; shock conditioning: 24 at 0.7 mA, 2-s duration, 10-s intervals, total of 4 min). hab, habituation. (B) Freezing behavior of Shock and BY mice during conditioning phase of socially transferred fear. (C) Freezing behavior of BY mice during retrieval phase of socially transferred fear. (D) Schematic of YFP and NpHR injection and experimental timeline of optogenetic stimulation in NAc or BLA. Light stimulation (~10 to 15 mW, 8-s on and 2-s off) periods are represented by yellow-green boxes. (E) Conditioning session with inhibition of ACC→NAc projections in YFP- and NpHR-BY mice during shock observation. (F) Freezing behavior of YFP- and NpHR-BY mice during retrieval phase. (G) First light-off session measuring mechanical sensitivity after NpHR inhibition of ACC→NAc projections during social transfer of pain in the same mice from (E) and (F). Dashed line represents mean baseline of all groups. (H) Conditioning session with inhibition of ACC→BLA projections in BY mice during shock observation. (I) Freezing behavior of YFP- and NpHR-BY mice during retrieval phase. (J) First light-off session measuring mechanical sensitivity after NpHR inhibition of ACC→BLA projections during social transfer of pain in the same mice from (H) and (I). Dashed line represents mean baseline of all groups. Data are means \pm SEM. Two-way repeated measures ANOVA with Holm Sidak post hoc tests comparing freezing to the first minute, where notation is the least significant P value of all comparisons [(B), (E), and (H)]; paired t test (C) or unpaired t test [(F) and (I)] comparing average baseline to average freezing during retrieval; or one-way ANOVA with Holm-Sidak post hoc tests [(G) and (J)]; * P < 0.05, ** P < 0.01, *** P < 0.001, **** P < 0.0001. All statistical measure details are presented in table S1D.



for ACC-to-NAc communication was established by demonstrating that bidirectional manipulation of activity in ACC→NAc inputs influences the acquisition of socially transferred pain but not the expression of mechanical sensitivity itself. Specifically, inhibiting this activity

during the 1-hour social interaction reduced hyperalgesia in BY mice, whereas increasing activity in ACC→NAc inputs prolonged the duration of the hyperalgesia evoked by the brief social interaction. ACC→NAc input activity was also necessary for the social

transfer of analgesia but not for the social transfer of fear, which requires activity in ACC projections to the BLA (36).

These results suggest that the ACC, which has been proposed to be a key brain area for mediating the emotional aspects of pain as

well as encoding information about the affective state of others (23, 30, 42), generates a specific and appropriate empathic behavioral response by accessing distinct downstream targets. The specificity of the neural circuit and behavioral response generated during socially transferred pain and fear may be, at least in part, due to the sensory modalities required for these two forms of social transfer.

The social transfer of pain does not require visual or auditory stimuli but can be generated by exposure to used bedding from mice experiencing pain, suggesting that olfactory cues are sufficient for this form of social transfer (9). By contrast, the social transfer of fear requires visual and/or auditory cues (3, 12). Further elucidation of the mechanisms by which this specificity in empathic neural and

behavioral responses occurs will be important for developing interventions that promote social context-appropriate empathic responses. Furthermore, a better understanding of the neural circuits mediating specific empathic responses will greatly facilitate the development of therapies that target pathological forms of empathy, or its absence, in a variety of neuropsychiatric disorders.

Fig. 5. ACC NAc projections regulate social transfer of analgesia.

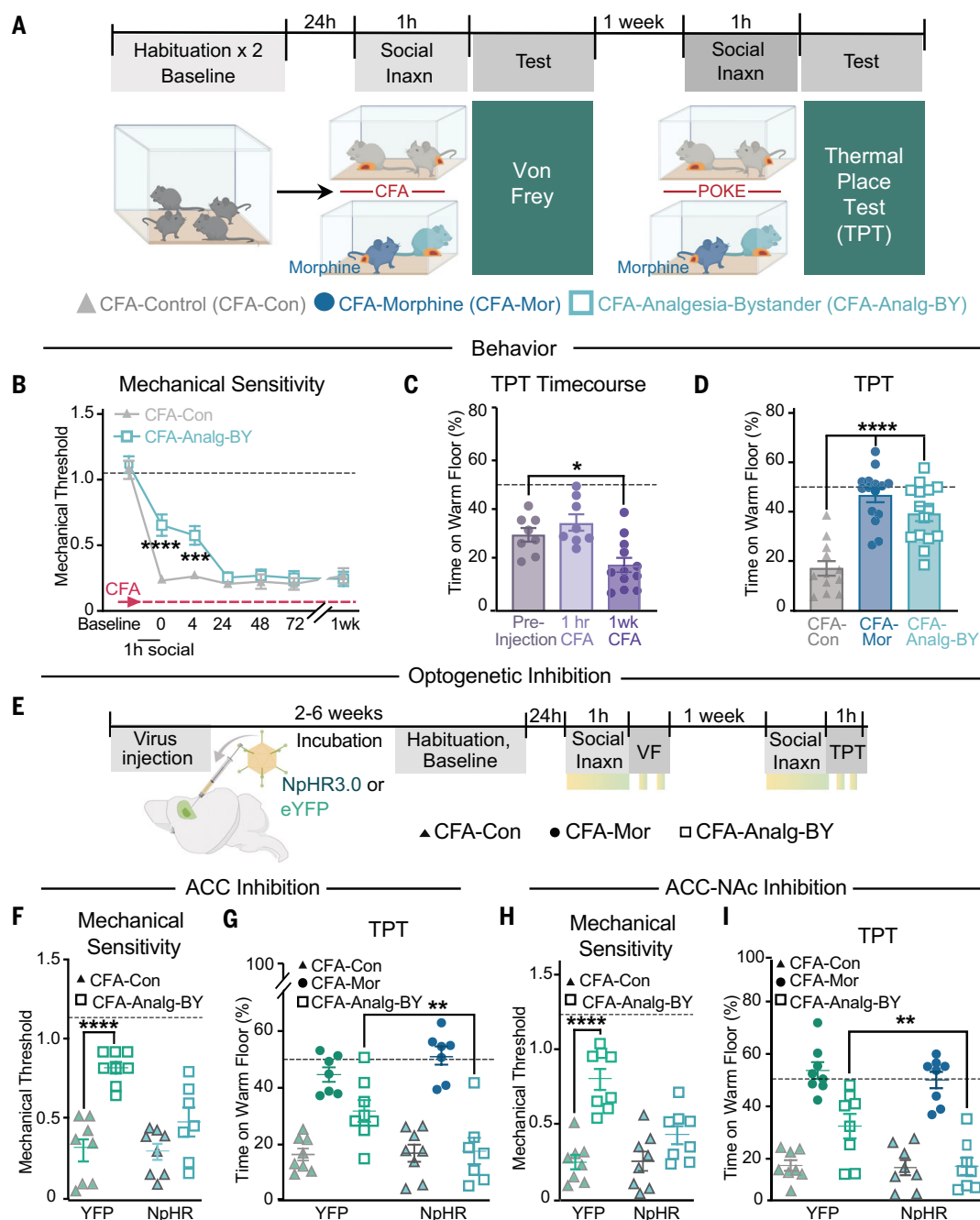
(A) Schematic of social transfer of analgesia protocol and timeline. Inaxn, interaction.

(B) Mechanical sensitivity at 0, 4, 24, 48, and 72 hours and 1 week after 1-hour social interaction in CFA-Con–CFA-Con pairs and CFA-Mor–CFA-Mor pairs. **(C)** Time on the warm (40°C) floor in the TPT before and 1 hour and 1 week (wk) after CFA injection. **(D)** Time on the warm (40°C) floor in the TPT immediately after the second 1-hour social transfer of analgesia, 1 week after CFA injection.

(E) Schematic of YFP and NpHR injection and optogenetic stimulation in ACC or NAc. Light stimulation (~10 to 15 mW, 8-s on and 2-s off) periods are represented by yellow-green boxes. **(F)** First light-off session measuring mechanical sensitivity after light stimulation of ACC in YFP- and NpHR-expressing CFA-Con and CFA-Analg-BY mice during social transfer of analgesia.

(G) Time on the warm (40°C) floor in the TPT after light stimulation of ACC in YFP- and NpHR-expressing CFA-Con, CFA-Mor, and CFA-Analg-BY mice during the second social transfer of analgesia test. **(H)** First light-off session measuring mechanical sensitivity after light stimulation of ACC→Nac projections in YFP- and NpHR-expressing CFA-Con and CFA-Analg-BY mice during social transfer of analgesia.

(I) Time on the warm (40°C) floor in the TPT after ACC→Nac light stimulation in YFP- and NpHR-expressing CFA-Con, CFA-Mor, and CFA-Analg-BY mice during the second social transfer of analgesia test. Data are means ± SEM; dashed lines in (B), (F), and (H) represent baseline thresholds for all groups; dashed lines in (C), (D), (G), and (I) represent 50% time on warm floor. Two-way repeated measures (B) or one-way [(C), (D), and (F) to (I)] ANOVA with Holm-Sidak post hoc tests comparing between groups; * $P < 0.05$, ** $P < 0.01$, *** $P < 0.001$, **** $P < 0.0001$. Not all significant post hoc analyses are displayed. All statistical measure details are presented in table S1E.



Historically, empathy, as defined by the ability to experience and share the emotions of others, was often considered to be a high level, affective-cognitive process experienced almost exclusively by humans (1, 2, 43). However, most investigators now accept that empathy can be deconstructed into specifiable, evolutionarily conserved components, many of which can be studied in rodents to elucidate their underlying neural mechanisms (3–5, 12, 44). Our results provide additional evidence that mice can rapidly and reliably adopt the sensory-affective state of a social partner, regardless of the valence of the information (pain, fear, or pain relief). Although it is conceivable that the behavioral responses of our BY mice reflect “imitative” or “mimicry” behavior (45) rather than “empathy,” several findings suggest that at least for the social transfer of pain and analgesia, the BY mice manifest changes in their behavior because they are experiencing an altered sensory-affective state. Importantly, the BY mice were tested using several different behavioral assays and did not always have direct visual access to their social partners during testing. In addition, control mice spent more time interacting with a BY mouse that had recently been exposed to a CFA mouse than with another control mouse, indicating that the BY mouse is in an altered affective state that is sufficient to attract control mice. Finally, as mentioned above, the social transfer of pain can be generated by bedding (9), which provides no opportunity for imitative or mimicry-like behavior.

The behavioral protocols we established are relatively easy to implement and generate multifaceted empathy-like behavior in mice, a species that offers many advantages for rapid, direct, and highly specific manipulation of neural circuit activity. Mechanistic findings from rodents and other experimentally accessible species provide new hypotheses that researchers studying human empathy can explore using tools such as neuromodulation methods and brain imaging. Advancing our understanding of the evolutionarily conserved brain mechanisms of empathy will, hopefully, also expedite the development of new interventions that promote the empathic social interactions that the world, apparently, desperately needs.

Materials and methods

Animals

All procedures were approved by the Stanford University Administrative Panel on Laboratory Animal Care in accordance with American Veterinary Medical Association Guidelines and the International Association for the Study of Pain. Unless otherwise specified, adult C57Bl/6J mice (strain 000664, Jackson Laboratory; aged 7 weeks at the start of experiments) were used. For targeted recombination in active populations (TRAP) experiments, we used male

and female second generation of *fos*-TRAP mice ($Fos^{2A-CreER}$; TRAP2, which were generously donated by the Luo lab at Stanford University), aged 7 to 16 weeks for all experiments. These mice were on a B6.129 background and, when necessary, were crossed with Ai14-TdTomato Cre-reporter mice (strain 007914, Jackson Laboratory) to visualize active neurons.

Housing

Mice were housed two to four per cage on a 12-hour light-dark cycle with food and water ad libitum. Cagemates were used in all experiments. At the start of each experiment, mice were housed four per cage. After the first day of experimental manipulation, mice were housed two per cage with experimentally matched cagemates (fig. S1).

Drugs

4-OHT (Sigma H6278) was prepared in a solution of castor and sunflower oil and administered intraperitoneally (50 mg/kg). Morphine was prepared in saline and administered subcutaneously (10 mg/kg, Sigma M8777). CFA (10 μ l, Sigma F5881) or capsaicin (10 μ g, Sigma M2808) was injected into the left hindpaw.

Viral reagents

Unless otherwise noted, all viral reagents were purchased from the Stanford Neuroscience Gene Vector and Virus Core. AAVDJ-*CaMKII α* -NpHR3.0-eYFP, AAVDJ-*CaMKII α* -eYFP, or AAVDJ-*CaMKII α* -Chr2-eYFP were used for all optogenetic experiments except those involving $FosCreER^{T2}$, in which AAVDJ-*CaMKII α* -DIO-NpHR3.0-eYFP or AAVDJ-*CaMKII α* -DIO-eYFP were used. For retrograde tracing, a 1:1 volume mixture of AAV-CAG-FLEX^{loxP}-TVA-mCherry and AAV-CAG-FLEX^{loxP}-RG was injected followed by EnvA-pseudotyped RVAG-GFP+EnvA (custom prep, L. Luo lab, 1.3×10^9 colony forming units/ml) into the same location 3 weeks later.

Stereotactic surgeries

All surgeries were conducted under aseptic conditions using a small animal digital stereotaxic instrument (David Kopf Instruments). Mice were anesthetized with isoflurane (5% induction, 1% maintenance), a small incision was made in the scalp, and burr holes were drilled in the brain surface at the appropriate stereotaxic coordinates [anterior-posterior (AP) and medial-lateral (ML) relative to bregma; dorsal-ventral (DV) relative to brain surface at target coordinate]: +0.98 AP, 0.278 ML, –0.78 DV for ACC; +0.98 AP, 1.12 ML, –4.15 DV for NAc. Viruses (0.3 μ l) were infused at a rate of 0.1 μ l/min using a glass micropipette connected to a Hamilton syringe by tubing backfilled with mineral oil. The injector tip was lowered an additional 0.1 mm below the planned injection site and then raised to the final coordinate before infusion to facilitate virus diffusion at the site

of injection, instead of along the needle track. After infusion, pipettes were raised 100 μ m for 5 min to allow for diffusion and then were removed slowly.

Optogenetic fibers (ferrules) were implanted ~10 to 50 μ m above the sites of interest, (0.98 AP, 0.278 ML, –0.3 DV unilaterally for ACC; 0.98 AP, 1.12 ML, –3.75 DV bilaterally for NAc core; –1.75 AP, 3.0 ML, –3.55 DV bilaterally for BLA). Ferrules were made in-house using 1.25-mm-diameter multimode ceramic ferrules (Thorlabs), 200- μ m fiber optic cable with numerical aperture (NA) 0.39 (Thorlabs), and blue dye epoxy (Fiber Instrument Sales). Ferrules were secured to the skull using miniature screws (thread size 00–90 \times 1/16, Antrin Miniature Specialties) and light-cured dental adhesive cement (Geristore A&B paste, DenMat). Mice recovered from anesthesia individually on a heating pad before being placed into group housing.

Monosynaptic tracing

Cell specific monosynaptic tracing studies were carried out as previously described (46), with minor modifications. A 1:1 volume mixture of AAV-CAG-FLEX^{loxP}-TVA-mCherry and AAV-CAG-FLEX^{loxP}-RG (200 nl) was injected into the NAc core of TRAP2 mice. One week later, mice were habituated in a behavior room and injected with saline intraperitoneally for two consecutive days and then injected with 4-OHT before the social interaction for 4 hours. Mice were then housed with treatment-matched cagemates for 3 weeks, at which time 200 nl of RVAG-GFP+EnvA was injected into the same location. Mice were subsequently housed for 1 week before sacrifice and tissue processing.

Optogenetic manipulations

For optogenetic photostimulation of Chr2, ferrules were connected to a 473-nm laser diode (OEM Laser Systems) through a FC/PC adaptor and a fiber optic rotary joint (Doric Lenses). Laser output was controlled using a Master-8 pulse stimulator (A.M.P.I.), which delivered 5-ms light pulses at 20 Hz. Light output through the optical fibers was adjusted to ~5 mW (somatic) or ~15 mW (terminals) using a digital power meter console (Thorlabs). For activation of NpHR3.0, the optical fiber was connected to a 532-nm laser diode (Shanghai Dream Lasers Technology Co, Ltd.) by a FC/PC adaptor and a fiber optic rotary joint (Doric Lenses). Laser output was again controlled using a Master-8 pulse stimulator (A.M.P.I.) and adjusted to ~5 mW (somatic) or ~10 to 15 mW (terminals). Mice received cycles of 8-s light on and 2-s light off. Mice were acclimated to optogenetic tethers during the acclimation-habituation periods before the test day.

Social transfer of pain

Mice were acclimated to the testing room for 40 min for 2 days before the beginning of the

experiments (see timeline in Fig. 1A). On the test day, mice were lightly restrained (Control, BY) or lightly restrained and injected with 10 μ l of an inflammatory medium, CFA, into the intraplantar surface of the left hind paw. CFA is known to rapidly and reliably produce long lasting localized inflammation (24, 25). Immediately after this quick handling, paired mice were placed into a clean housing cage (without food or water) for a 1-hour social interaction, at which time they were subjected to mechanical threshold testing and then the other requisite behavioral testing (Fig. 1A). For time course experiments, after the initial behavioral assays, mice were housed as pairs with treatment-matched cagemates (and intermittently subjected to mechanical threshold assays). On the second test session in thesecond week, mice were lightly restrained (Control, BY) or lightly restrained and pricked with a 26-gauge needle on the surface of the left hind paw (CFA) and subjected to behavioral testing. For experiments with optogenetic manipulations, mice were tethered to optogenetic cables during acclimation.

Mechanical sensitivity

All assays were performed without knowledge of the experimental manipulation or viral injection performed on each individual subject in a given group. However, control mice were run in separate cohorts to limit exposure to mice that had been given noxious stimuli, because even brief exposure to CFA and BY mice caused significant variance in mechanical thresholds (e.g., fig. S2, A and B). Furthermore, in CFA mice, substantial swelling in the CFA-injected hindpaw occurred several hours after injection and often made blinding to this group impossible at later time points. Responses (withdrawal, shaking, or licking the paw) to (1 to 2 s) mechanical stimulation of the plantar surface of the left hindpaw were determined with von Frey hairs (0.01- to 2-g plastic fibers, Touch Test) using the up-down technique (26). This method uses stimulus oscillation around the response threshold to determine the median 50% threshold of response. Mice were allowed to acclimate to homemade plexiglass enclosures on top of a homemade wire testing rack for 20 min on 2 days before the start of the experiment and for 10 to 30 min before each test session. The testing rack was located within each testing room and illuminated with a dim lamp. Unless otherwise noted, mechanical sensitivity was assessed before treatment exposure (baseline, represented by a dotted line “—” on mechanical sensitivity graphs), and then testing occurred 24 hours later. For time-course experiments and certain optogenetic experiments, testing occurred at 0, 4, 24, 48, and 72 hours and 1 week after social interaction. For optogenetic experiments, mechanical thresholds were taken with the light off and the light on in the following pattern: off, on, off, on. The

light was turned on or off for the duration of each threshold test, which took less than 1 min per mouse. Data are displayed as the first light-off session (Figs. 3, B, D, and F; 4, G and J; and 5, F and H) followed by the average of the light-on and light-off sessions (Fig. 3, C, E, and G).

Thermal place test

The TPT occurred on a dual hot-cold plate (Bioseb, BIO-T2CT) with opaque plexiglass walls surrounding the two compartments (13-in long; 3-in wide; 9.5-in high). One floor and side of the chamber was set to room temperature (30°C), and the other side and floor was set to (40°C). Mice were allowed to freely explore the chamber for 10 min; data are displayed as an average time spent during minutes 6 to 10, because mice were acclimating to the new environment during minutes 1 to 5. Pilot behavioral experiments determined that mice do not show thermal place aversion to the warm area (40°C) versus the reference area (30°C) 1 hour after CFA injection but do display an avoidance of the warm floor 1 week after CFA injection (Fig. 5C). Additionally, pilot tests determined that mice could not be placed on the hot plate repeatedly, as they quickly learned to avoid the warm floor almost entirely.

Tail immersion

Mice were tested for thermal nociceptive sensitivity using the heat-evoked tail withdrawal reflex. Two days before the first test session, mice were habituated to handling (light restraint in a soft cloth) and the tip of their tail (5 cm from the end) was immersed into room temperature water. On the test days, mice were lightly restrained, and the tail was submerged into 46°C water to measure the latency of the response (flicking the tail out of water) using a stopwatch. Two tail withdrawal measurements were taken 10 min apart and averaged for a single data point for each animal.

Emotional discrimination

Briefly [described in detail in (27)], mice were habituated to the enclosures for 10 min, 3 days before the test day. Test observer mice were allowed to explore the entire chamber during habituation (free of other mice), whereas CFA, BY, and Neutral “demonstrator” mice were habituated for 10 min under the wire cups. The enclosure included walls (35.5 cm by 23.5 cm by 19 cm) and a separator (11 cm by 14 cm) made with black plexiglass and two black cylindrical wire pencil cups (10.5 cm in height, bottom diameter 10.2 cm, bars spaced 1 cm apart). A plastic cup was placed on the top of the wire cups to prevent the observer mice from climbing. On the test day, mice were subjected to a 1-hour social interaction to create CFA, BY, and Control pairs (interaction was the same as that used in social transfer paradigms).

Immediately after the social interaction, pairs of mice were placed under the cups: either a BY mouse paired with a Control mouse, a CFA mouse paired with a Control mouse, or two Control mice. An age and sex-matched stranger test mouse was allowed to explore the entire chamber for 6 min. The sessions were video recorded and manually scored with a stopwatch after the fact by an experimenter blind to the treatment conditions.

Social transfer of analgesia

On the test day, mice were lightly restrained and injected with 10 μ l of CFA into the intraplantar surface of the left hind paw, immediately followed by a subcutaneous injection of either 10 mg/kg morphine (CFA-MOR) or saline (CFA-Control or CFA-Analg-BY). Pairs of mice were then placed into a clean housing cage for 1 hour, immediately followed by mechanical testing (Fig. 5A). After mechanical testing, mice were separated and housed for 1 week with treatment-matched cagemates, before being subjected to a second set of assays. On this second test day, mice were lightly restrained and pricked with a 26-gauge needle on the surface of the left hind paw, followed by subcutaneous injection of either 10 mg/kg morphine (CFA-Mor) or saline (CFA-Control or CFA-Analg-BY). Mice were then placed back in their housing cage with their previous partner for 1 hour, followed by mechanical testing and the TPT. After the social transfer and behavioral test, all mice were separated and housed with treatment-matched cagemates (fig. S1). For optogenetic experiments, laser stimulation was given during the entire social interaction as described above and during every other minute during the TPT.

Observational fear response

Observational fear response assays were performed as described previously (19), with slight modifications. Two fear-conditioning shock chambers, made by different manufacturers, in two entirely separate rooms were used as the two separate contexts (context A: Ugo Bassile passive avoidance chamber, and context B: Med Associate self-administration chambers with shock floor additions). To enhance the magnitude of the social transfer of fear (36, 44), 24 hours before the social transfer procedure (day 1; Fig. 4A), BY mice were administered a shock experience by being placed in one of the fear-conditioning chambers (context A; Fig. 4A) for 5 min at which time they received two unpredicted, uncued, footshocks (0.4 mA, for 2 s, 1-min interval) and then transferred back to their home cage with treatment matched cagemates. The following day (day 2), a naive mouse was placed in the other fear-conditioning chamber (context B) while a BY mouse was placed in an adjacent homemade plexiglass observation chamber, which allowed for the

communication of visual, auditory, and olfactory cues through a transparent, perforated plexiglass divider. After a 5-min habituation period, the naïve mouse received 24 unpredicted, uncued, footshocks (0.7 mA, for 2 s, 10-s intervals over 4 min). The entire session was recorded with a high-definition camera (Logitech), and the time spent freezing was scored manually using a stopwatch. Mice were then housed in pairs for 24 hours with treatment-matched cagemates. The following day (day 3), contextual observational fear memory was assessed by placing the BY mice back into the observation chamber in the same context (context B) for 10 min.

For optogenetic manipulations, fiber optic patch-cords were connected to the BY mice before transfer to the observation chamber on days 2 and 3. On day 2, the laser was turned on for the entire 4-min shock period. On day 3, the laser was turned off and on every other minute. One week after completion of the social transfer of fear experiments, shocked and BY mice were subjected to the social transfer of pain test (Fig. 4D). There was no difference in baseline mechanical thresholds between shocked and BY mice, which were counterbalanced into CFA and BY groups.

Real-time place preference test

A 35.5-cm-by-23.5-cm-by-19-cm chamber was divided into two compartments by a partial barrier. The left and right compartments had different visual cues, and the side initially paired with stimulation was randomly assigned each day. Optical stimulation was controlled by a computer running Biobserve software, which tracked animal position and triggered light delivery by video tracking location. Initially, the mouse was placed in the nonstimulated compartment with the rest of the arena closed off. The mouse was free to explore the entire arena for the remainder of the test. Every time the mouse crossed to the stimulation-paired side of the chamber, pulsed light was delivered (473-nm laser, 5-ms light pulses at 20 Hz, ~10- to 15-mW output) until the mouse crossed back into the other side. Immediately after the initial test, a reversal test was conducted and the side paired with stimulation was switched; there was no interruption between the initial and the reversal phases of the experiment. The average time of the initial and reversal sessions were used for analysis.

General histological procedures, cell counting, and imaging

Mice were deeply anesthetized with sodium pentobarbital, transcardially flushed with cold phosphate-buffered saline (PBS), and perfused with 4% paraformaldehyde-PBS. Brains were removed, postfixed for 24 hours, and then cryoprotected in 20% sucrose-PBS for 24 hours followed by 30% sucrose for 24 hours, at which

point they were either transferred to PBS for storage or immediately sectioned on a cryostat (40- μ m slices). TRAP2;Ai14 brain slices did not require immunohistochemistry to visualize TdTomato-positive neurons, which were manually counted by a researcher blind to experimental condition. Sections containing 12 brain regions of interest were selected for analysis. Brain regions were defined using the Mouse Brain Atlas (47) parameters. Photos from each slice were overlaid onto corresponding brain atlas slices, and all TdTomato-positive cells within the designated brain region were manually counted by a researcher blind to experimental condition. Averages for each region were determined from across three to eight slices from six to nine mice in each group. Both male and female TRAP2 mice were used, because no sex dependent differences were detected ($P > 0.05$).

For localization of viral injections, sections were rinsed between steps with PBS and blocked in 5% normal donkey serum-PBS (The Jackson Laboratory) for 45 min. The tissue was then incubated overnight with 1:1000 rabbit anti-GFP antibody (Aves, GFP-1020). This was followed by 1-hour incubations with Alexa Fluor 488-labeled secondary antibodies (raised in donkey, Invitrogen catalog number A-11055). Finally, slices were washed with PBS, mounted on charged slides, and coverslipped with Prolong Gold (Invitrogen). Viral infusions were considered accurate when neuronal expression of the virus was limited to the boundaries of the chosen brain region [as defined by (47)]. When visualization of the virus was not possible or spread of the virus was beyond the designated target, data were not included. This occurred in less than 5% of the injected mice.

For analysis of monosynaptic rabies tracing, sections were processed by immunohistochemistry for GFP (described above), injection location was verified in the NAc core by presence of GFP and mCherry fluorescence, and cells were manually counted from three slices throughout the ACC from three mice in each group (CFA, BY).

REFERENCES AND NOTES

- M. L. Hoffman, Developmental synthesis of affect and cognition and its implications for altruistic motivation. *Dev. Psychol.* **11**, 607–622 (1975). doi: [10.1037/0012-1649.11.5.607](https://doi.org/10.1037/0012-1649.11.5.607)
- F. B. M. de Waal, Putting the altruism back into altruism: The evolution of empathy. *Annu. Rev. Psychol.* **59**, 279–300 (2008). doi: [10.1146/annurev.psych.59.103006.093625](https://doi.org/10.1146/annurev.psych.59.103006.093625); pmid: [17550343](https://pubmed.ncbi.nlm.nih.gov/17550343/)
- J. B. Panksepp, G. P. Lahvis, Rodent empathy and affective neuroscience. *Neurosci. Biobehav. Rev.* **35**, 1864–1875 (2011). doi: [10.1016/j.neubiorev.2011.05.013](https://doi.org/10.1016/j.neubiorev.2011.05.013); pmid: [21672550](https://pubmed.ncbi.nlm.nih.gov/21672550/)
- S. Sivaseelvachandran, E. L. Acland, S. Abdallah, L. J. Martin, Behavioral and mechanistic insight into rodent empathy. *Neurosci. Biobehav. Rev.* **91**, 130–137 (2018). doi: [10.1016/j.neubiorev.2016.06.007](https://doi.org/10.1016/j.neubiorev.2016.06.007); pmid: [27311631](https://pubmed.ncbi.nlm.nih.gov/27311631/)
- S. Keum et al., Variability in empathic fear response among 11 inbred strains of mice. *Genes Brain Behav.* **15**, 231–242 (2016). doi: [10.1111/gbb.12278](https://doi.org/10.1111/gbb.12278); pmid: [26690560](https://pubmed.ncbi.nlm.nih.gov/26690560/)
- D. J. Langford et al., Social modulation of pain as evidence for empathy in mice. *Science* **312**, 1967–1970 (2006). doi: [10.1126/science.1128322](https://doi.org/10.1126/science.1128322); pmid: [16809545](https://pubmed.ncbi.nlm.nih.gov/16809545/)

- D. Baptista-de-Souza et al., Mice undergoing neuropathic pain induce anxiogenic-like effects and hypernociception in cagemates. *Behav. Pharmacol.* **26**, 664–672 (2015). doi: [10.1097/FBP.0000000000000170](https://doi.org/10.1097/FBP.0000000000000170); pmid: [26258589](https://pubmed.ncbi.nlm.nih.gov/26258589/)
- Z. Li et al., Social interaction with a cagemate in pain facilitates subsequent spinal nociception via activation of the medial prefrontal cortex in rats. *Pain* **155**, 1253–1261 (2014). doi: [10.1016/j.pain.2014.03.019](https://doi.org/10.1016/j.pain.2014.03.019); pmid: [24699208](https://pubmed.ncbi.nlm.nih.gov/24699208/)
- M. L. Smith, C. M. Hostetler, M. M. Heinricher, A. E. Ryabinin, Social transfer of pain in mice. *Sci. Adv.* **2**, e1600855 (2016). doi: [10.1126/sciadv.1600855](https://doi.org/10.1126/sciadv.1600855); pmid: [27774512](https://pubmed.ncbi.nlm.nih.gov/27774512/)
- M. L. Smith, A. T. Walcott, M. M. Heinricher, A. E. Ryabinin, Anterior cingulate cortex contributes to alcohol withdrawal-induced and socially transferred hyperalgesia. *eNeuro* **4**, ENEURO.0087-17.2017 (2017). doi: [10.1523/NEURO.0087-17.2017](https://doi.org/10.1523/NEURO.0087-17.2017); pmid: [28785727](https://pubmed.ncbi.nlm.nih.gov/28785727/)
- Y.-F. Lu et al., Social interaction with a cagemate in pain increases allogrooming and induces pain hypersensitivity in the observer rats. *Neurosci. Lett.* **662**, 385–388 (2018). doi: [10.1016/j.neulet.2017.10.063](https://doi.org/10.1016/j.neulet.2017.10.063); pmid: [29102786](https://pubmed.ncbi.nlm.nih.gov/29102786/)
- A. Kim, S. Keum, H.-S. Shin, Observational fear behavior in rodents as a model for empathy. *Genes Brain Behav.* **18**, e12521 (2019). doi: [10.1111/gbb.12521](https://doi.org/10.1111/gbb.12521); pmid: [30264490](https://pubmed.ncbi.nlm.nih.gov/30264490/)
- J. P. Burkett et al., Oxytocin-dependent consolation behavior in rodents. *Science* **351**, 375–378 (2016). doi: [10.1126/science.aac4785](https://doi.org/10.1126/science.aac4785); pmid: [26798013](https://pubmed.ncbi.nlm.nih.gov/26798013/)
- H. Ueno et al., Helping-like behaviour in mice towards conspecifics constrained inside tubes. *Sci. Rep.* **9**, 5817 (2019). doi: [10.1038/s41598-019-42290-y](https://doi.org/10.1038/s41598-019-42290-y); pmid: [30967573](https://pubmed.ncbi.nlm.nih.gov/30967573/)
- I. Ben-Ami Bartal, J. Decety, P. Mason, Empathy and pro-social behavior in rats. *Science* **334**, 1427–1430 (2011). doi: [10.1126/science.1210789](https://doi.org/10.1126/science.1210789); pmid: [22158823](https://pubmed.ncbi.nlm.nih.gov/22158823/)
- C. Lamm, J. Decety, T. Singer, Meta-analytic evidence for common and distinct neural networks associated with directly experienced pain and empathy for pain. *Neuroimage* **54**, 2492–2502 (2011). doi: [10.1016/j.neuroimage.2010.10.014](https://doi.org/10.1016/j.neuroimage.2010.10.014); pmid: [20946964](https://pubmed.ncbi.nlm.nih.gov/20946964/)
- I. Timmers et al., Is empathy for pain unique in its neural correlates? A meta-analysis of neuroimaging studies of empathy. *Front. Behav. Neurosci.* **12**, 289 (2018). doi: [10.3389/fnbeh.2018.00289](https://doi.org/10.3389/fnbeh.2018.00289); pmid: [30542272](https://pubmed.ncbi.nlm.nih.gov/30542272/)
- P. L. Jackson, E. Brunet, A. N. Meltzoff, J. Decety, Empathy examined through the neural mechanisms involved in imagining how I feel versus how you feel pain. *Neuropsychologia* **44**, 752–761 (2006). doi: [10.1016/j.neuropsychologia.2005.07.015](https://doi.org/10.1016/j.neuropsychologia.2005.07.015); pmid: [16140345](https://pubmed.ncbi.nlm.nih.gov/16140345/)
- D. Jeon et al., Observational fear learning involves affective pain system and Ca_v1.2 Ca²⁺ channels in ACC. *Nat. Neurosci.* **13**, 482–488 (2010). doi: [10.1038/nn.2504](https://doi.org/10.1038/nn.2504); pmid: [20190743](https://pubmed.ncbi.nlm.nih.gov/20190743/)
- M. Carrillo et al., Emotional mirror neurons in the rat's anterior cingulate cortex. *Curr. Biol.* **29**, 1301–1312.e6 (2019). doi: [10.1016/j.cub.2019.03.024](https://doi.org/10.1016/j.cub.2019.03.024); pmid: [30982647](https://pubmed.ncbi.nlm.nih.gov/30982647/)
- C. Fillinger, I. Yalcin, M. Barrot, P. Veinante, Efferents of anterior cingulate areas 24a and 24b and midcingulate areas 24a' and 24b' in the mouse. *Brain Struct. Funct.* **223**, 1747–1778 (2018). doi: [10.1007/s00429-017-1585-x](https://doi.org/10.1007/s00429-017-1585-x); pmid: [29209804](https://pubmed.ncbi.nlm.nih.gov/29209804/)
- P. L. Jackson, A. N. Meltzoff, J. Decety, How do we perceive the pain of others? A window into the neural processes involved in empathy. *Neuroimage* **24**, 771–779 (2005). doi: [10.1016/j.neuroimage.2004.09.006](https://doi.org/10.1016/j.neuroimage.2004.09.006); pmid: [15652312](https://pubmed.ncbi.nlm.nih.gov/15652312/)
- F. L. Stevens, R. A. Hurley, K. H. Taber, Anterior cingulate cortex: Unique role in cognition and emotion. *J. Neuropsychiatry Clin. Neurosci.* **23**, 121–125 (2011). doi: [10.1176/jnp.23.2.jnp121](https://doi.org/10.1176/jnp.23.2.jnp121); pmid: [21677237](https://pubmed.ncbi.nlm.nih.gov/21677237/)
- A. A. Larson, D. R. Brown, S. el-Atrash, M. M. Walser, Pain threshold changes in adjuvant-induced inflammation: A possible model of chronic pain in the mouse. *Pharmacol. Biochem. Behav.* **24**, 49–53 (1986). doi: [10.1016/0091-3057\(86\)90043-2](https://doi.org/10.1016/0091-3057(86)90043-2); pmid: [3945666](https://pubmed.ncbi.nlm.nih.gov/3945666/)
- K. Ren, R. Dubner, Inflammatory models of pain and hyperalgesia. *ILAR J.* **40**, 111–118 (1999). doi: [10.1093/ilar.40.3.111](https://doi.org/10.1093/ilar.40.3.111); pmid: [11406689](https://pubmed.ncbi.nlm.nih.gov/11406689/)
- S. R. Chaplan, F. W. Bach, J. W. Pogrel, J. M. Chung, T. L. Yaksh, Quantitative assessment of tactile allodynia in the rat paw. *J. Neurosci. Methods* **53**, 55–63 (1994). doi: [10.1016/0165-0270\(94\)90144-9](https://doi.org/10.1016/0165-0270(94)90144-9); pmid: [7990513](https://pubmed.ncbi.nlm.nih.gov/7990513/)
- V. Ferretti et al., Oxytocin signaling in the central amygdala modulates emotion discrimination in mice. *Curr. Biol.* **29**, 1938–1953.e6 (2019). doi: [10.1016/j.cub.2019.04.070](https://doi.org/10.1016/j.cub.2019.04.070); pmid: [31178317](https://pubmed.ncbi.nlm.nih.gov/31178317/)
- C. J. Guenther, K. Miyamichi, H. H. Yang, H. C. Heller, L. Luo, Permanent genetic access to transiently active neurons via TRAP: Targeted recombination in active populations. *Neuron* **78**, 773–784 (2013). doi: [10.1016/j.neuron.2013.03.025](https://doi.org/10.1016/j.neuron.2013.03.025); pmid: [23764283](https://pubmed.ncbi.nlm.nih.gov/23764283/)

29. W. E. Allen *et al.*, Thirst-associated preoptic neurons encode an aversive motivational drive. *Science* **357**, 1149–1155 (2017). doi: [10.1126/science.aan6747](https://doi.org/10.1126/science.aan6747); pmid: [28912243](https://pubmed.ncbi.nlm.nih.gov/28912243/)
30. M. A. J. Apps, M. F. S. Rushworth, S. W. C. Chang, The anterior cingulate gyrus and social cognition: Tracking the motivation of others. *Neuron* **90**, 692–707 (2016). doi: [10.1016/j.neuron.2016.04.018](https://doi.org/10.1016/j.neuron.2016.04.018); pmid: [27196973](https://pubmed.ncbi.nlm.nih.gov/27196973/)
31. J. J. Walsh *et al.*, 5-HT release in nucleus accumbens rescues social deficits in mouse autism model. *Nature* **560**, 589–594 (2018). doi: [10.1038/s41586-018-0416-4](https://doi.org/10.1038/s41586-018-0416-4); pmid: [30089910](https://pubmed.ncbi.nlm.nih.gov/30089910/)
32. L. W. Hung *et al.*, Gating of social reward by oxytocin in the ventral tegmental area. *Science* **357**, 1406–1411 (2017). doi: [10.1126/science.aan4994](https://doi.org/10.1126/science.aan4994); pmid: [28963257](https://pubmed.ncbi.nlm.nih.gov/28963257/)
33. M. A. J. Apps, P. L. Lockwood, J. H. Balsters, The role of the midcingulate cortex in monitoring others' decisions. *Front. Neurosci.* **7**, 251 (2013). doi: [10.3389/fnins.2013.00251](https://doi.org/10.3389/fnins.2013.00251); pmid: [24391534](https://pubmed.ncbi.nlm.nih.gov/24391534/)
34. E. M. Callaway, L. Luo, Monosynaptic circuit tracing with glycoprotein-deleted rabies viruses. *J. Neurosci.* **35**, 8979–8985 (2015). doi: [10.1523/JNEUROSCI.0409-15.2015](https://doi.org/10.1523/JNEUROSCI.0409-15.2015); pmid: [26085623](https://pubmed.ncbi.nlm.nih.gov/26085623/)
35. E. J. Kim, M. W. Jacobs, T. Ito-Cole, E. M. Callaway, Improved monosynaptic neural circuit tracing using engineered rabies virus glycoproteins. *Cell Rep.* **15**, 692–699 (2016). doi: [10.1016/j.celrep.2016.03.067](https://doi.org/10.1016/j.celrep.2016.03.067); pmid: [27149846](https://pubmed.ncbi.nlm.nih.gov/27149846/)
36. S. A. Allsop *et al.*, Corticoamygdala transfer of socially derived information gates observational learning. *Cell* **173**, 1329–1342.e18 (2018). doi: [10.1016/j.cell.2018.04.004](https://doi.org/10.1016/j.cell.2018.04.004); pmid: [29731170](https://pubmed.ncbi.nlm.nih.gov/29731170/)
37. F. B. M. de Waal, S. D. Preston, Mammalian empathy: Behavioural manifestations and neural basis. *Nat. Rev. Neurosci.* **18**, 498–509 (2017). doi: [10.1038/nrn.2017.72](https://doi.org/10.1038/nrn.2017.72); pmid: [28655877](https://pubmed.ncbi.nlm.nih.gov/28655877/)
38. M. Watanabe, M. Narita, Brain reward circuit and pain. *Adv. Exp. Med. Biol.* **1099**, 201–210 (2018). doi: [10.1007/978-981-13-1756-9_17](https://doi.org/10.1007/978-981-13-1756-9_17); pmid: [30306526](https://pubmed.ncbi.nlm.nih.gov/30306526/)
39. H. N. Harris, Y. B. Peng, Evidence and explanation for the involvement of the nucleus accumbens in pain processing. *Neural Regen. Res.* **15**, 597–605 (2020). doi: [10.4103/1673-5374.266909](https://doi.org/10.4103/1673-5374.266909); pmid: [31638081](https://pubmed.ncbi.nlm.nih.gov/31638081/)
40. A. M. Klawonn, R. C. Malenka, Nucleus accumbens modulation in reward and aversion. *Cold Spring Harb. Symp. Quant. Biol.* **83**, 119–129 (2018). doi: [10.1101/sqb.2018.83.037457](https://doi.org/10.1101/sqb.2018.83.037457); pmid: [30674650](https://pubmed.ncbi.nlm.nih.gov/30674650/)
41. N. Schwartz *et al.*, Decreased motivation during chronic pain requires long-term depression in the nucleus accumbens. *Science* **345**, 535–542 (2014). doi: [10.1126/science.1253994](https://doi.org/10.1126/science.1253994); pmid: [25082697](https://pubmed.ncbi.nlm.nih.gov/25082697/)
42. T. Singer *et al.*, Empathy for pain involves the affective but not sensory components of pain. *Science* **303**, 1157–1162 (2004). doi: [10.1126/science.1093535](https://doi.org/10.1126/science.1093535); pmid: [14976305](https://pubmed.ncbi.nlm.nih.gov/14976305/)
43. S. D. Preston, F. B. M. de Waal, Empathy: Its ultimate and proximate bases. *Behav. Brain Sci.* **25**, 1–20 (2002). doi: [10.1017/S0140525X02000018](https://doi.org/10.1017/S0140525X02000018); pmid: [12625087](https://pubmed.ncbi.nlm.nih.gov/12625087/)
44. K. Z. Meyza, I. B.-A. Barta, M. H. Monfils, J. B. Panksepp, E. Knapka, The roots of empathy: Through the lens of rodent models. *Neurosci. Biobehav. Rev.* **76**, 216–234 (2017). doi: [10.1016/j.neubiorev.2016.10.028](https://doi.org/10.1016/j.neubiorev.2016.10.028); pmid: [27825924](https://pubmed.ncbi.nlm.nih.gov/27825924/)
45. H. Ueno *et al.*, Conformity-like behaviour in mice observing the freezing of other mice: A model of empathy. *BMC Neurosci.* **21**, 19 (2020). doi: [10.1186/s12868-020-00566-4](https://doi.org/10.1186/s12868-020-00566-4); pmid: [32357830](https://pubmed.ncbi.nlm.nih.gov/32357830/)
46. K. T. Beier *et al.*, Rabies screen reveals GPe control of cocaine-triggered plasticity. *Nature* **549**, 345–350 (2017). doi: [10.1038/nature23888](https://doi.org/10.1038/nature23888); pmid: [28902833](https://pubmed.ncbi.nlm.nih.gov/28902833/)
47. G. Paxinos, K. B. J. Franklin, *Paxinos and Franklin's the Mouse Brain in Stereotaxic Coordinates* (Academic Press, 2012).

ACKNOWLEDGMENTS

We thank the Luo lab for generously providing the TRAP2 breeding pairs, M. Lenail for contributing to the cell counting in the TRAP2 analysis, the Sudhof lab for access to fear conditioning equipment, and B. Bentzley for aid in modifying the behavioral chambers used in the social transfer of fear experiments. **Funding:** This work was supported by the UCSF Dolby Family Center for Mood Disorders. M.L.S. was supported by the National Institute on Drug Abuse (T32DA035165-06) and a Stanford University School of Medicine Deans Fellowship. **Author contributions:** All studies were conceptualized and designed by M.L.S., N.A., and R.C.M. Experiments were performed and analyzed by M.L.S. and N.A. The paper was written by M.L.S. and R.C.M., with editorial comments by N.A. **Competing interests:** R.C.M. is a cofounder and scientific advisor of MapLight Therapeutics. R.C.M. is also on the scientific advisory board of Cerevance, Inc.; The Brave Neuroscience Co.; AZ Therapies; and Cognition Therapeutics. **Data and materials availability:** All data are available in the main text or the supplementary materials.

SUPPLEMENTARY MATERIALS

science.sciencemag.org/content/371/6525/153/suppl/DC1

Figs. S1 to S6

Table S1

MDAR Reproducibility Checklist

[View/request a protocol for this paper from Bio-protocol.](#)

12 August 2020; accepted 5 November 2020

10.1126/science.abe3040

Anterior cingulate inputs to nucleus accumbens control the social transfer of pain and analgesia

Monique L. Smith, Naoyuki Asada and Robert C. Malenka

Science **371** (6525), 153-159.
DOI: 10.1126/science.abe3040

Social transmission of pain and relief

In mice, both pain and fear can be transferred by short social contact from one animal to a bystander. Neurons in a brain region called the anterior cingulate cortex in the bystander animal mediate these transfers. However, the specific anterior cingulate projections involved in such empathy-related behaviors are unknown. Smith *et al.* found that projections from the anterior cingulate cortex to the nucleus accumbens are necessary for the social transfer of pain in mice (see the Perspective by Klein and Gogolla). Fear, however, was mediated by projections from the anterior cingulate cortex to the basolateral amygdala. Interestingly, in animals with pain, analgesia can also be transferred socially.

Science, this issue p. 153; see also p. 122

ARTICLE TOOLS

<http://science.sciencemag.org/content/371/6525/153>

SUPPLEMENTARY MATERIALS

<http://science.sciencemag.org/content/suppl/2021/01/06/371.6525.153.DC1>

RELATED CONTENT

<http://science.sciencemag.org/content/sci/371/6525/122.full>

REFERENCES

This article cites 46 articles, 11 of which you can access for free
<http://science.sciencemag.org/content/371/6525/153#BIBL>

PERMISSIONS

<http://www.sciencemag.org/help/reprints-and-permissions>

Use of this article is subject to the [Terms of Service](#)

Science (print ISSN 0036-8075; online ISSN 1095-9203) is published by the American Association for the Advancement of Science, 1200 New York Avenue NW, Washington, DC 20005. The title *Science* is a registered trademark of AAAS.

Copyright © 2021, American Association for the Advancement of Science